Radio Science, Volume 24, Number 3, Pages 393–406, May–June 1989

Interpretation of layered structure in mesospheric VHF echoes induced by an inertia gravity wave

Yoshikazu Muraoka

Department of Physics, Hyogo College of Medicine, Nishinomiya, Hyogo, Japan

Takuya Sugiyama

Department of Physics, Kyoto University, Kyoto, Japan

Toru Sato,[1] *Toshitaka Tsuda, Shoichiro Fukao, and Susumu Kato*

Radio Atmospheric Science Center, Kyoto University, Uji, Kyoto, Japan

(Received April 26, 1988; revised December 5, 1988; accepted January 3, 1989.)

A remarkable layered structure of mesospheric VHF echo was observed on September 20, 1985, in the experiments with the middle and upper atmosphere (MU) radar at Shigaraki, Japan. The echoing layers were seen at the heights where the static stability in the atmosphere increases owing to the simultaneously observed inertia gravity wave motion. In this paper we show that the height profile of the observed echo power can be interpreted as due to the modulation of a mean gradient of potential refractive index by the gravity wave under the assumption of a height independent spectrum of turbulent irregularities. It is then shown that the enhancement of the observed echo agrees well with sharp gradients of electron density which are formed through the reactions between chemical species vertically transported by the wave.

1. INTRODUCTION

It has been widely accepted that the radar backscatter at VHF from the middle atmosphere can be explained by two distinct mechanisms: Fresnel reflections from horizontally stratified, stable laminae of sharp gradients in the refractive index and volume scattering from turbulent irregularities [e.g., *Röttger*, 1987]. At the same time, many observational studies have shown that the contribution from the two mechanisms coexists in the enhanced VHF echoes obtained at vertical incidence [*Röttger and Liu*, 1978; *Gage and Green*, 1978; *Fukao et al.*, 1979; *Röttger et al.*, 1979]. Attempts to fill the gap between theory and observation have been made in the last several years [e.g., *Gage and Balsley*, 1980; *Röttger*, 1980; *Doviak and Zrnic'*, 1984; *Gage et al.*, 1985; *Hocking*, 1987].

Gage et al. [1981] have introduced irregularities into the Fresnel reflection model to explain the anisotropic VHF echoes from stable regions in the stratosphere. Such an idea has been known as Fresnel irregularities in the partial reflection at MF [e.g., *Austin and Manson*, 1969]. The extended model is now called Fresnel scattering because it assumes reflection from a group of laminae with random vertical displacements within the radar's resolution range [*Hocking and Röttger*, 1983; *Gage et al.*, 1985]. Using this model, *Gage et al.* [1981, 1985] have shown that the magnitude of the observed echo depends on the mean gradient of potential refractive index, and so on the static stability in the stratosphere. On the other hand, *Doviak and Zrnic'* [1984] have shown that the aspect sensitivity in the observed echo can be interpreted as due to scattering from anisotropic irregularities. Furthermore, they conclude that the Fresnel scattering model is simply another approach to solve the problem of scattering from turbulent irregularities. However, it seems that the Fresnel scattering model gives a physically comprehensible description of backscattered echo in the vertical incidence.

[1]Now at Department of Electrical Engineering, Kyoto University, Yoshida, Japan.

Paper number 89RS00039.
0048-6604/89/89RS-00039$08.00

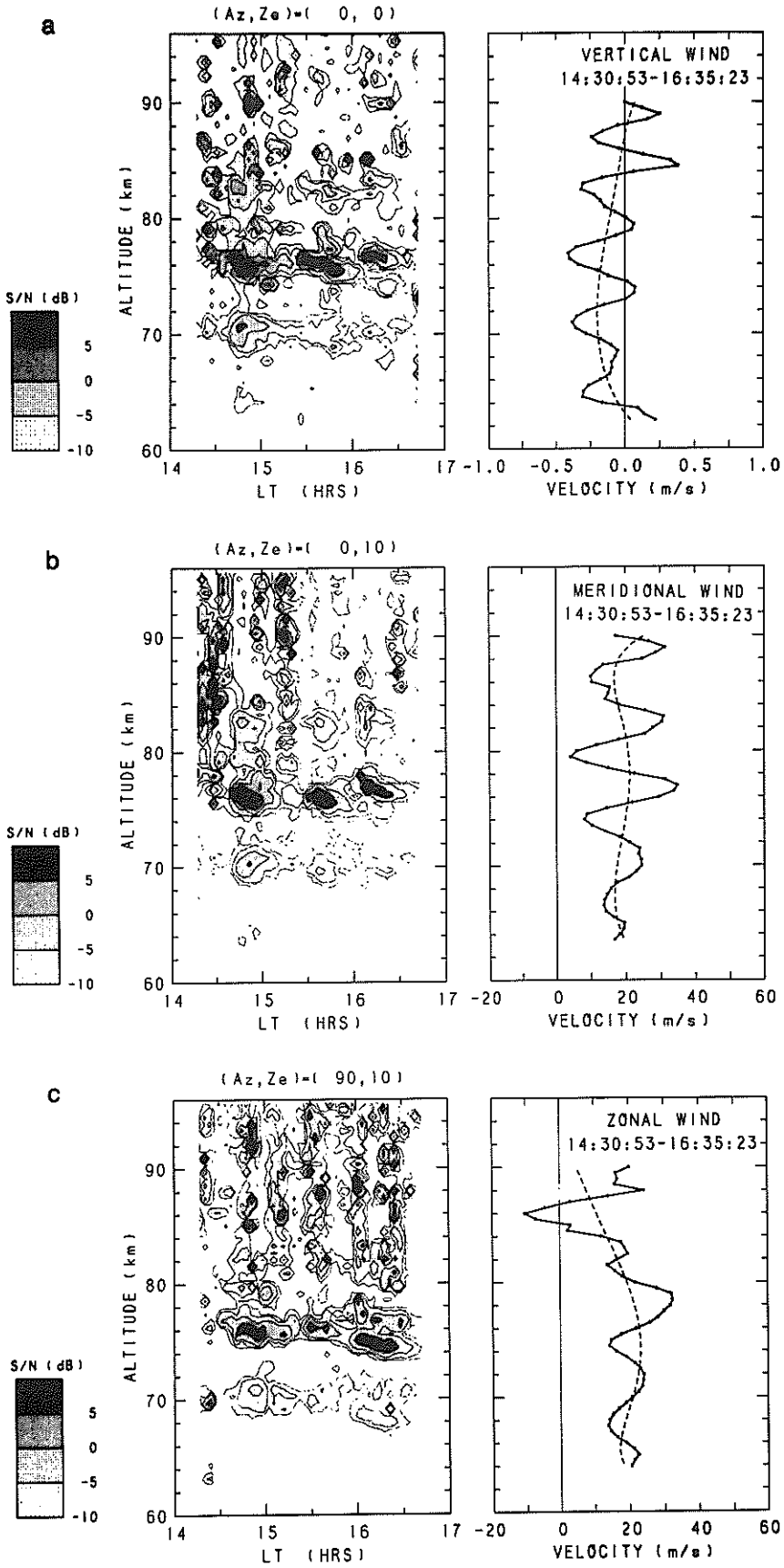
a
(Az,Ze)=(0, 0)
VERTICAL WIND
14:30:53-16:35:23
S/N (dB)
5
0
-5
-10
ALTITUDE (km)
90
80
70
60
14
15
16
17
LT (HRS)
-1.0
-0.5
0.0
0.5
1.0
VELOCITY (m/s)
b
(Az,Ze)=(0,10)
MERIDIONAL WIND
14:30:53-16:35:23
S/N (dB)
5
0
-5
-10
ALTITUDE (km)
90
80
70
60
14
15
16
17
LT (HRS)
-20
0
20
40
60
VELOCITY (m/s)
c
(Az,Ze)=(90,10)
ZONAL WIND
14:30:53-16:35:23
S/N (dB)
5
0
-5
-10
ALTITUDE (km)
90
80
70
60
14
15
16
17
LT (HRS)
-20
0
20
40
60
VELOCITY (m/s)

As for the mesosphere, several studies on the layered structure in the backscattered VHF echo have appeared in the last several years [e.g., *Balsley et al.*, 1983; *Smith et al.*, 1986; *Yamamoto et al.*, 1987; *Kelley and Ulwick*, 1988]. In these studies the observed echoes have been discussed on the basis of turbulent scattering, and the enhanced echoes have been connected with turbulence generated, for example, by the unstable breakdown of tide and gravity waves. On the other hand, *Muraoka et al.* [1988*a*] have recently shown that a multilayered structure in the observed echo was connected with stable regions formed by an inertial gravity wave motion. This result suggests that we may explain the observed echo in terms of a mean gradient of potential refractive index in the mesosphere, as *Gage et al.* [1985] could in the stratosphere.

In this paper we briefly summarize some features of the mesospheric echo observed with the middle and upper atmosphere (MU) radar and compare the result with the Fresnel scattering model. This is followed by the discussion of the cause of the echo scattering in the mesosphere. We also discuss the response of electrons to the observed long-period gravity wave, considering the influence of the wave on the dynamical and chemical processes in the mesosphere. Our ultimate purpose is to clarify the contribution of a mean gradient of potential refractive index to the radar backscatter at VHF from the mesosphere.

2. MU RADAR OBSERVATION OF MESOSPHERIC ECHOES

The MU radar is a monostatic pulse radar with an active phased array system, operating at a frequency of 46.5 MHz with about 1 MW peak radiated power. The antenna is a circular array with an aperture of 8330 m^2. Details of the system may be found in the papers of *Fukao et al.* [1985*a*, *b*]. In recent mesospheric observations with the MU radar at Shigaraki (34.9°N, 136.1°E), Japan, we have shown that a triple-layered structure in the received echo was well correlated with an inertia gravity wave motion [*Muraoka et al.*, 1987; 1988*a*]. For the purpose of that experiment of measuring three components of wind velocity, the main beam of the radar had been transmitted in the vertical and two off-vertical directions, by turns. All the backscattered echoes had been obtained with a pulse modulated by a 16-element complementary code with subpulse width of 4 μs ($\Delta r = 0.60$ km). The received echo signals had been coherently integrated over 20 pulses of transmission. The power spectra calculated with a 128-point fast Fourier transform method had been further averaged over about 3 min.

A comparison between height profiles of mesospheric echo and the related wind velocity is reproduced in Figure 1. This figure shows that a triple echoing layer is seen in agreement with the downward and northward velocity perturbations due to a monochromatic wave motion with a vertical wavelength of 6 km. In the wind profiles, a decrease in the horizontal component of the wave amplitude is seen above 80 km, while the amplitude increases exponentially below this altitude with height. This wave breaking has been explaind as due to the occurrence of local unstable state in the wave field [*Muraoka et al.*, 1988*b*]. In this connection it is noted that the echo power in the highest layer ($\sim$83 km) was not so enhanced in comparison with the others. The wave parameters have been estimated from the polarization relations between the observed wind velocity perturbations [*Muraoka et al.*, 1987]. They are summarized in Table 1 together with the simultaneously obtained quantities of the background mean atmosphere. Note that the wave was almost stationary ($c = 0$) and was an internal mode of inertia gravity waves ($f \leqq \omega \ll \omega_{BO}$). Using the dispersion and polarization relations of the wave with these parameters and the measured wind data, *Muraoka et al.* [1988*a*] have further estimated the static stability defined as $\omega_B^2 = g(\partial/\partial z)(\ln \theta)$, where g is the acceleration of gravity, and θ is the potential temperature. In Figure 2, the height changes of the local static stability (normalized by the mean value, ω_{BO}^2) are compared with the height profile of the averaged echo obtained at vertical incidence during the period 1430–1635 LT on September 20, 1985. The solid and dashed lines in Figure 2*b* indicate the changes in the static stability estimated respectively from the measured wind data

Fig. 1. (Opposite) (*a*) Time-height contour of mesospheric echo intensity in the vertical radar beam (left) and averaged profile of the vertical component of wind velocity (right) observed in the period 1430–1635 LT on September 20, 1985. The contour levels are given at 5 dB intervals. The positive value of the wind velocity indicates upward motion. The dashed curve indicates the background mean flow. (*b*) Echo intensity in the beam deflected northward by 10° from the zenith and meridional component wind profile. The positive value of the wind velocity indicates northward motion. (*c*) Echo intensity in the beam deflected eastward by 10° from the zenith and zonal component wind profile. The positive value of the wind velocity indicates eastward motion.

TABLE 1. Summary of Parameters on Observed Gravity Wave Motion and Mean Atmosphere in the Mesosphere

Quantity	Notation	Value
Wave Field		
Vertical wavelength	$\lambda_z = 2\pi/\lvert m\rvert$	6 km
Horizontal wavelength	$\lambda_x = 2\pi/k$	400 km
Period	$2\pi/\omega$	5.6 h
Vertical phase velocity	ω/m	30 cm s^{-1} downward
Horizontal phase velocity	ω/k	20 m s^{-1} southward
Ratio of the intrinsic to inertial frequency	f/ω	0.3
Doppler-shifted horizontal phase velocity	$c = \omega/k + \bar{u}$	0 m s^{-1}
*Background Mean Field**		
Meridional wind velocity	$\bar{u}$	20 ms s^{-1} northward
Vertical wind velocity	$\bar{w}$	20 cm s^{-1} downward
Brunt-Väisälä frequency	ω_{BO}	0.021 s^{-1}
Scale height	H	6.2 km
Temperature	$\bar{T}$	210 K

*Evaluated around 75 km altitude.

and from the wave parameters together with the assumption of exponentially growing wave amplitude. Figure 2 shows that the magnitude of the observed echo is well correlated with the static stability in the wave field. While the magnitude of the peak echo power increased with height below 80 km, it was considerably reduced around 83 km. In this connection it is noted in Figure 2*b* that the static stability in the actual wave field, indicated by the solid line, was reduced because of the wave breaking shown in Figure 1. Therefore the reduction of echo power appears to be connected with the breakdown of the observed wave.

3. INTERPRETATION OF THE MESOSPHERIC ECHO PROFILE

We have shown that the static stability in the gravity wave field was well correlated with the strength of VHF echo backscattered from the mesosphere. In the stratosphere the stability dependence of the echo power was observed by *Gage and Green* [1978] and has been explained by *Gage et al.* [1981, 1985], who introduced a mean gradient of potential refractive index in the Fresnel scattering model. On the analogy of their results we apply the Fresnel scattering model to the mesospheric heights to explain our observational results.

3.1. *Fresnel scattering model in the mesosphere*

In the Fresnel scattering model the backscattered power P_r which arises from a partial reflection process is given by the radar equation,

$$P_r = (\alpha^2 P_T A_e^2/4\lambda_R^2 r^2)\lvert \rho_R \rvert^2 \tag{1}$$

where P_T is transmitted power per pulse, A_e is effective antenna area, α is an efficiency factor, r is the range, λ_R is radar wavelength, and $\lvert \rho_R \rvert^2$ is a power reflection coefficient which depends on the refractivity structure in the volume of the atmosphere in question [e.g., *Balsley and Gage*, 1980]. The voltage reflection coefficient ρ_R for the vertical incidence in a layer with the vertical extent of Δr is given in the general form

$$\rho_R(z) = \frac{1}{2}\int_{z-\Delta r/2}^{z+\Delta r/2} \frac{dn}{dz'} e^{-2ik_R Z'}\, dz' \tag{2}$$

where n is the total refractive index and $k_R = 2\pi/\lambda_R$ [e.g., *Wait*, 1970]. Although (2) is originally for a continuous wave, it is regarded as an approximation of the reflection coefficient for a pulse length Δr [*Gage et al.*, 1985].

To evaluate the magnitude of (2) in the mesosphere, we first consider the refractivity structure at the mesospheric heights according to the idea of Fresnel scattering. It is well known that the ionospheric component of refractive index in the mesosphere can be approximated as

$$n = 1 - (2\pi r_e/k_R^2)N \tag{3}$$

where N is electron number density and r_e is the classical electron radius. In the Fresnel scattering process it is assumed that there are many thin horizontally stratified layers in the height range of the incident pulse length. The pulse incident on a layer is reflected partially because the layers are transversely coherent within the horizontal extent of a Fresnel zone at least. At the same time it is assumed that each layer undergoes a random vertical displacement due to either turbulence or small-scale waves [*Hocking and Röttger*, 1983; *Gage et al.*, 1985]. Imagine an air parcel in the layer displaced vertically a small distance $\Delta z = z - z_0$ from its equilibrium level z_0 by

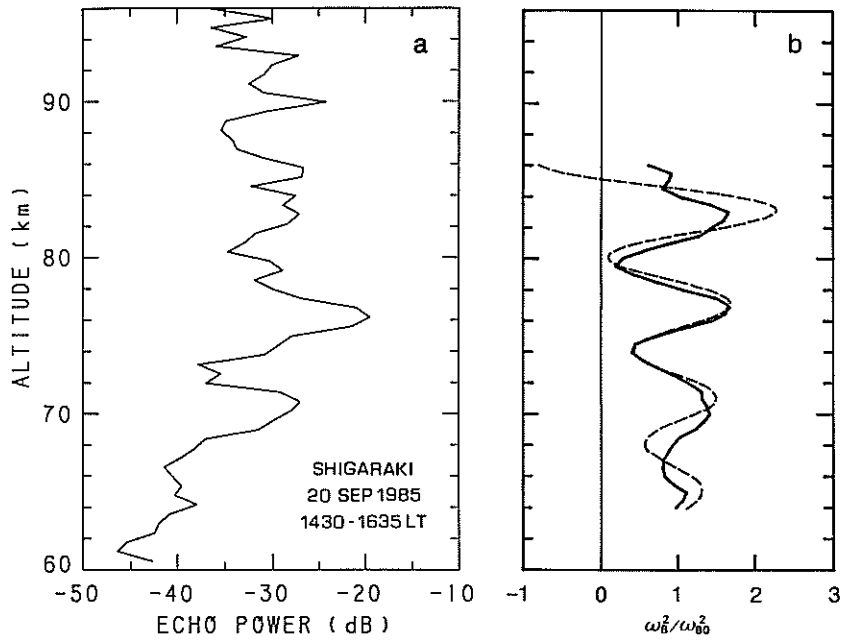

Fig. 2. Comparison between height profiles of (*a*) an averaged echo power for the vertical beam shown in Figure 1*a* and (*b*) normalized total static stability (ω_B^2/ω_{B0}^2). The solid line in Figure 2*b* indicates a height change of ω_B^2/ω_{B0}^2 estimated with parameters of the observed wave summarized in Table 1 [cf. *Muraoka et al.*, 1988*a*]. The dashed curve indicates the height change for a modeled wave with an exponential growth rate.

such irregularities. Then, we may represent the refractive index in the displaced parcel as

$$n_P(Z) = n(z) + M\Delta z \tag{4}$$

where n_P and n are the refractive indices in the parcel and in the environmental atmosphere, respectively, and M denotes a rate of change of the refractive index including the adiabatic change in the displaced parcel. Following *Tatarski* [1961] and *Ottersten* [1969], we call M the mean gradient of potential refractive index in a stratified atmosphere with no irregularity. *Gage et al.* [1985] have shown that M is determined primarily by its dry air part of the total refractive index in the upper troposphere and in the stratosphere. In the mesosphere it is easily shown that M is determined by the contribution from free electrons:

$$M_e = -\frac{\partial n}{\partial N}\left(\frac{dN}{dz} + \frac{N}{\gamma p}\frac{dp}{dz}\right) \tag{5}$$

where p is atmospheric pressure and γ is the ratio of the specific heats. In Appendix A we prove this connection using the parcel method which *Thrane and Grandal* [1981] have used to describe the fluctuation of ion density in the D region. The manner of derivation is different from that given by *Hocking* [1985], although both yield the same result. Note that the total derivatives with respect to z in (5) denote the mean gradients of N and p in the atmosphere across the turbulent layer.

Substituting M_e for M in (4) and using the result, we can rewrite the voltage reflection coefficient given by (2) as

$$\rho_R = 1ik_R \int_{z-\Delta r/2}^{z+\Delta r/2} n_P(z')e^{-2ik_R z'}\,dz'$$
$$\fallingdotseq ik_R M_e \int_{z-\Delta r/2}^{z+\Delta r/2} \Delta z(z')e^{-2ik_R z'}\,dz' \tag{6}$$

In the derivation of (6) we simply regarded n and M_e in (4) as constant in the height range of the pulse length, since Δr is smaller than the scale length of electron density in the mesosphere and the vertical wavelength of the gravity wave considered here. Note that (6) gives the reflection coefficient observed at height z for a single pulse. If we take into account the procedure of actual radar echo measurement, it is convenient to introduce an averaged reflection coefficient for an array of pulses. In the usual statistical

approach [cf. *Liu*, 1983] the averaged reflection coefficient is given by

$$\bar{\rho}_R = ik_R M_e \int_{z-\Delta r/2}^{z+\Delta r/2} \langle \Delta z(z') \rangle e^{-2ik_R z'} \, dz' \tag{7}$$

where $\langle \ \rangle$ denotes an ensemble average. Here we assume that the vertical displacement is due to completely random irregularities: $\langle \Delta z \rangle = 0$ and that the irregularity varies slowly with height within the scale of Δr. Although the value of (7) is zero in this case, the averaged power reflection coefficient defined as

$$\overline{|\rho_R|^2} \equiv \overline{\rho_R \rho_R^*} = k_R^2 M_e^2 \int_{-\Delta r/2}^{\Delta r/2} dz \int_{-\infty}^{+\infty} ds \cdot \langle \Delta z(z) \Delta z(z+s) \rangle e^{-2ik_R s} \tag{8}$$

has a definite value. Equation (8) is further rewritten as

$$\overline{|\rho_R|^2} = k_R^2 M_e^2 \, \Delta r E_\xi(2k_R) \tag{9}$$

by introducing the spectrum of the vertical displacement:

$$E_\xi(k) \equiv \int_{-\infty}^{+\infty} ds \, \langle \Delta z(z) \Delta z(z+s) \rangle e^{-iks} \tag{10}$$

Note that the correlation length of the irregularities is assumed to be much less than Δr in (8) [cf. *Liu*, 1983].

Replacing r with z in (1) and substituting (9) into (1), we see that the backscattered echo power in the vertical incidence can be rewritten as

$$P_r = (\pi^2 \alpha^2 P_T A_e^2 \Delta r / \lambda_R^4 z^2)[E_\xi(2k_R) M_e^2] \tag{11}$$

The formulation of the echo power given by (11) is consistent, for example, with that derived from the concept of isotropic turbulent scattering, because also in the latter model the received echo power depends on M and the intensity of turbulence [cf., *Gage and Balsley*, 1980; *Hocking*, 1985]. To investigate the height dependence of P_r, it is necessary to consider the height dependence of each factor in (11). Since

$$P_r \propto E_\xi M_e^2 / z^2 \propto \frac{E_\xi}{z^2} \left(\frac{dN}{dz} + \frac{N}{\gamma p} \frac{dp}{dz} \right)^2 \tag{12}$$

it is clear that P_r is dependent on the height profile of electron number density in addition to E_ξ. We assume hereafter that E_ξ is independent of altitude in order to examine the influence of the observed monochromatic inertia gravity wave on the structure of M_e in the mesosphere.

3.2. *Modulation of mean gradient of potential refractive index due to gravity waves*

In this subsection we describe the mesospheric structure modulated by a vertically propagating monochromatic gravity wave. Following our observational results (compare Table 1), we consider here an inertia gravity wave with the intrinsic frequency ω such that

$$f \leqq \omega \ll \omega_{B0} \tag{13}$$

where f and ω_{B0} are the inertial and Brunt-Väisälä frequencies, respectively, in the background mean atmosphere. Assuming no wave dissipation in the vertical propagation, we can represent the wave-induced vertical wind velocity in the form

$$w' = w_0(z) e^{z/2H} \exp \{ik(x - ct) + imz\} \tag{14}$$

where k and m are the horizontal and vertical wave number, respectively, c is the horizontal phase velocity, and H is the scale height of the background mean atmosphere. Hereafter we denote the wave-induced quantities by primes. Note that the intrinsic frequency ω with respect to the background mean flow $\bar{u}$ is defined as

$$\omega \equiv k(c - \bar{u}) \tag{15}$$

The other wave-induced winds can also be written explicitly by using the appropriate polarization relations:

$$u' = -(m/k)w' \tag{16}$$

$$v' = -(if/\omega)u' \tag{17}$$

As the monochromatic gravity wave propagates vertically, it breaks down at the height where the amplitude satisfies the condition of convective instability: $u'/(c - \bar{u}) \geqq 1$ [*Hodges*, 1967; *Lindzen*, 1981]. Assuming that $u' = c - \bar{u}$ at height z_B, we obtain

$$w'(z_B) = -\omega/m \tag{18}$$

with the aid of (15) and (16). Note that the wave observed in our experiment no longer grew in amplitude exponentially above z_B [*Muraoka et al.*, 1988*b*]. Using (18), we can rewrite (14) as

$$w'(z) = -(\omega/m) e^{(z - z_B)/2H} e^{i(\phi)} \tag{19}$$

where $\phi = k(x - ct) + mz$. Here we assume that $\phi = 0$ at $z = z_B$.

In the gravity wave field we can divide the atmospheric pressure in (5) into two parts as

$$p = \bar{p} + p' \tag{20}$$

where $\bar{p}$ and p' are the background mean and wave-induced perturbation pressures. Then, the ratio of the perturbation to the mean is given by

$$p'/\bar{p} = -(\omega_{B0}^2/m\omega gH)w' \tag{21}$$

The change of electron number density in the gravity wave field is described by the continuity equation,

$$\partial N/\partial t + \nabla \cdot (N\mathbf{v}) = Q - L \tag{22}$$

where $\mathbf{v}$ is the macroscopic background and wave-induced flow and Q and L are respectively the volume production and loss rates of N. When an air parcel is vertically displaced in the mesosphere for some reason, the electron number density is changed from its equilibrium value. The time scale for the relaxation to photochemical equilibrium within the parcel has been studied by *Hill and Bowhill* [1979]. The study showed that the relaxation time is shorter than the period of the gravity wave considered here. When such a long-period gravity wave exists, the change of N is maintained primarily through the perturbation of Q and L due to the wave. In Appendix B we prove this connection by using a simplified chemical model in the lower D region. Thus the electron number density in (5) can be also divided into two parts as

$$N = \bar{N} + N' \tag{23}$$

where $\bar{N}$ and N' are the background mean and wave-induced perturbation electron number densities, respectively. Here we may assume that

$$\bar{N} = N_0(z_0)e^{(z-z_0)/L} \tag{24}$$

where L is a scale length for the background electron profile. On the basis of the consideration in Appendix B, we may represent the wave-modulated electron number density in the form

$$N'/\bar{N} = -(iw'/\omega H)F_R \tag{25}$$

where F_R denotes the response of electron to the wave. *Sugiyama* [1988] has discussed that in the D region the electron perturbation due to long-period gravity waves is generally given in the same form as in (25). F_R becomes complex if the time scale for the electron loss process due to the recombination is not much shorter than the period of the wave considered here.

Substituting (19), (24), and (25) into (23), and using differentials of (20) and (23) with respect to z, we find that (5) can be rewritten as

$$M_e = \frac{2\pi r_e \bar{N}}{k_R^2}\left(\frac{1}{L}+\frac{1}{\gamma H}\right)[1-\beta|F_R|e^{(z-z_B)/2H}\cos(\phi+\varepsilon)] \tag{26}$$

in terms of real variables, where

$$\beta = \frac{(1 + 1/m^2H'^2)^{1/2}}{H[(1/L) + (1/\gamma H)]} \tag{27}$$

$$\tan\varepsilon = \frac{\mathrm{Im}\,(F_R) - [\mathrm{Re}\,(F_R)/mH']}{\mathrm{Re}\,(F_R) + [\mathrm{Im}\,(F_R)/mH']} \tag{28}$$

$$1/H' = (1/L) + (1/\gamma H) + (1/2H) \tag{29}$$

In the derivation of (26), we neglected p' because the ratio of $p'/\bar{p}$ given by (21) is smaller than an order of 0.01 for the wave motion considered here (compare Table 1).

3.3. *Parameterization of Fresnel scattering model*

Substituting (26) for M_e in (11), we can estimate the echo power backscattered from the mesosphere in the case that a monochromatic inertia gravity wave propagates vertically into the mesosphere. In order to compare the height profile of the mesospheric echo power measured in our experiment with that obtained from the present model, we define a normalized received power S_v as

$$S_v = \frac{2C\lambda_R^2}{\pi r_e \alpha^2 P_r A_e^2 \Delta r} P_r\left[\frac{z\ (\mathrm{km})}{60\ (\mathrm{km})}\right]^2 \tag{30}$$

where C is an arbitrary number introduced for convenience. Combining (30) with (11), we obtain

$$S_v = \frac{CE_\xi(2k_R)}{[60\ (\mathrm{km})]^2}\left(\frac{1}{L}+\frac{1}{\gamma H}\right)^2 \bar{N}^2 \cdot [1-\beta|F_R|e^{(z-z_B)/2H}\cos(\phi+\varepsilon)]^2 \tag{31}$$

In the model calculation with (31) we use the wave and mean atmospheric parameters which have been estimated consistently from the simultaneously measured wind data (compare Table 1). In the following section we compare the result of the model calculation with that obtained from the echo power measurement. However, we restrict the comparison to the heights below 80 km because the observed gravity wave did not grow exponentially in amplitude above that height because of wave breaking [cf. *Muraoka et al.*, 1988*b*].

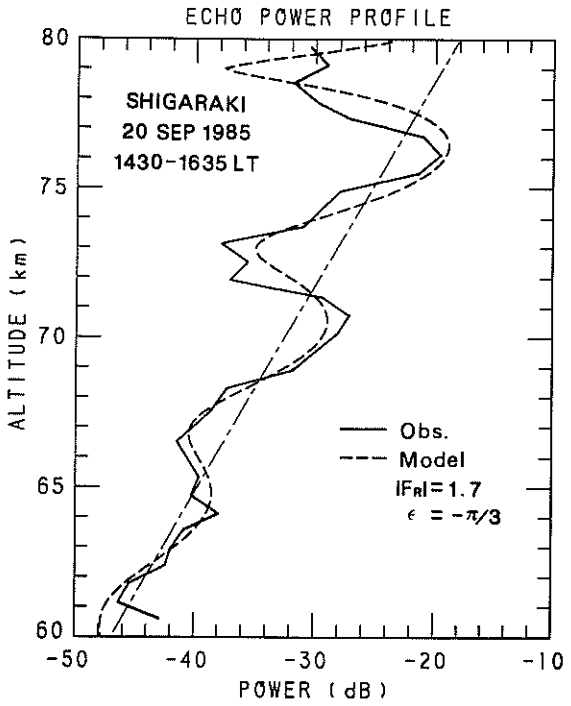

Fig. 3. Comparison of estimated and observed height profiles of normalized mesospheric echo power for 1430–1635 LT on September 20, 1985.

4. COMPARISON OF MU RADAR OBSERVATION WITH FRESNEL SCATTERING MODEL

Figure 3 shows a comparison between the height profile of mesospheric echo power which was measured with the MU radar on September 20, 1985, and that which was estimated from the Fresnel scattering model. The observed profile, indicated by the solid line in the figure, is an average of about 2 hours of data which were taken during the period 1430–1635 LT. The dot-dashed line in Figure 3 shows an echo profile estimated from (31) with the parameters of N_0 (80 km) = 1.0×10^3 cm^{-3} and $L = 6.0$ km, which is for the case of no wave motion. The assumed background mean electron number density profile was taken so as to be consistent with the currently accepted one in the middle latitude [e.g., *Brasseur and Solomon*, 1986]. In addition, the value of H was taken from our observational results (Table 1). The dashed line in Figure 3 shows an echo profile estimated from (31) for the case that the observed monochromatic gravity wave exists. The parameters of the wave were also taken from our observational results (Table 1) together with $z_B = 79$ km [cf. *Muraoka et al.*, 1988*b*]. As for the response factor, we adopted the values of $|F_R| = 1.7$ and $\varepsilon = -\pi/3$, in order to fit the model profile to the observed one. The resultant model profile shows an overall agreement with the observed one in the magnitude and shape. In Figure 4 we show the estimated height profiles of electron number density modulated in the gravity wave field and of the wave-induced vertical wind velocity. It is clear from the comparison of Figures 3 and 4 that the altitudes indicating maxima of the observed echo power coincide well with those indicating maxima of the vertical gradient of the wave-modulated electron number density. This suggests that in the mesosphere the mean gradient of electron number density contributes dominantly to the backscattering of VHF radar beam.

Another comparison between the measured and estimated echo power profiles is shown in Figure 5. The measured profile, indicated by the solid line, is an average of about 2 hours of data taken during the period 1202–1406 LT on September 20, 1985. Note that these data were taken just after the local noon, about 2.5 hours earlier than those of Figure 3. Considering the difference of the solar zenith angle between the two periods, we adopted the values of N_0 (80 km) = 2.0×10^3 cm^{-3} and $L = 6.0$ km for the background mean electron density profile. The resulting model profile for the case of no wave motion is shown by the dot-dashed line in Figure 5. The dashed line in Figure 5 shows an echo power profile

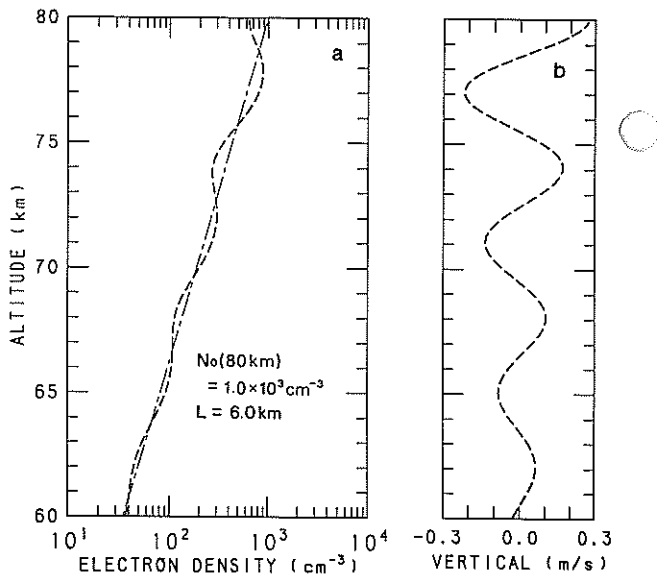

Fig. 4. Height profiles of (*a*) electron density and (*b*) vertical wind perturbations estimated from the observed echo power and gravity wind motion summarized in Table 1.

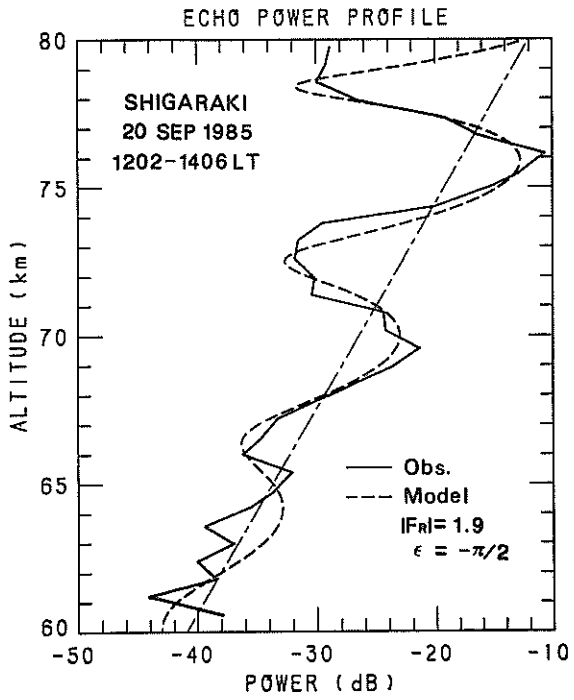

Fig. 5. Same as Figure 3 except for comparison for 1202–1406 LT on September 20, 1985.

for the case that the observed gravity wave exists. As for the parameters of the wave, we again used the values shown in Table 1 together with $z_B = 81$ km [cf. *Muraoka et al.*, 1988*b*]. In addition we adopted the values of $|F_R| = 1.9$ and $\varepsilon = -\pi/2$ for the response factor to fit the estimated profile to the observed one. As a result, the overall agreement in the magnitude and shape of the observed and modeled profiles is good also in this case, although no enhancement of the observed echo was seen below 65 km where the amplitude of the observed wave was still small. A comparison between Figures 5 and 6 shows that the altitudes indicating maxima of the observed echo power coincide well with those indicating maxima of the vertical gradient of electron number density. This suggests that the contribution of the mean gradient of electron number density is dominant in the VHF echo backscattered from the mesosphere.

5. DISCUSSION

We have shown that the Fresnel scattering model is effective in explaining the enhancement of VHF echo in the mesosphere as well as in the stratosphere. In our model calculation we considered the modulation of the mean gradient of potential refractive index due to the simultaneously observed gravity wave while we assumed the spectrum of irregularities to be height independent. As a result, the comparison between the observation and the model showed a good agreement. This indicates that the assumption about irregularities may be justified in this case, although it was initially introduced to simplify our model calculation. In the stratosphere, *Gage et al.* [1985] have assumed that the spectrum of irregularities has a height dependence of $e^{-z/H}$, based on the altitude dependence of horizontal kinetic energy observed in the lower stratosphere at Poker Flat [*Balsley and Garello*, 1985]. At the same time they have suggested that the spectrum of irregularities would become independent of altitude if the irregularities are due to small-scale gravity waves and the growth of their amplitude with height is limited by some wave-breaking process. Recently, *Smith et al.* [1987] pointed out that the saturation of such small-scale gravity waves in the middle atmosphere can be expected from the universality seen in a number of observations on a spectrum of velocity fluctuations. Consequently there is a strong possibility that the spectrum of irregularities is usually independent of height in the mesosphere because of the saturation of small-scale gravity waves. Thus we may conclude that the enhancement of mesospheric echo in our

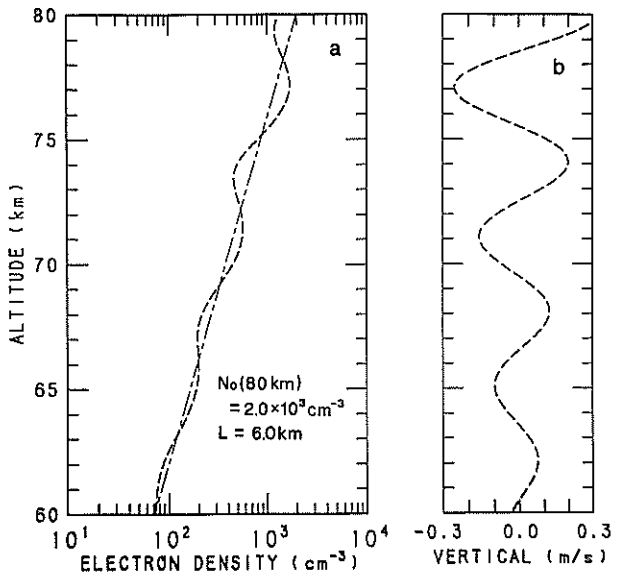

Fig. 6. Same as Figure 4 except for profiles concerning Figure 5.

experiment is due to the modulation of the mean gradient of potential refractive index by the gravity wave with the long vertical scale.

We restricted the comparison between the observation and the model calculation to below 80 km, because the observed wave was no longer growing exponentially in amplitude above 80 km. The wave dissipation was due to the unstable breakdown of the wave [*Muraoka et al.*, 1988*b*]. In addition, it is widely believed that the wave breaking is responsible for the generation of turbulence [*Lindzen*, 1981]. In connection with the wave breaking we have shown in Figure 2 that the echo power was significantly reduced in the highest layer (~83 km). This suggests that the generation of turbulence resulting from the wave breaking is not directly connected with the echo enhancement. Moreover, this strongly suggests that the reduction of echo power arises from a change in the vertical structure of the wave-modulated mean gradient of potential refractive index, whose cause is attributed to the wave breaking. This may be endorsed by the fact that the static stability dependence of the echo power is still conserved above 80 km in spite of the stability reduction owing to the wave breaking as shown in Figure 2.

In the evaluation of the mean gradient of potential refractive index in the observed gravity wave field, we used the wave and mean atmospheric parameters consistently estimated from the simultaneously measured wind data. In addition, we made assumptions about the mean electron density profile and the response of electron density to the gravity wave. The two observed echo power profiles with a time lag of about 2.5 hours required different values of the parameters for the background electron density and the electron response factor. Since the concentrations of electrons, ions, and some neutral species in the *D* region are strongly controlled by the solar radiation flux, the difference in the parameters of the model profile is probably related to the change in the solar zenith angle during the measurement.

With respect to the electron response factor used in the model calculation, we discuss the validity of the choice in Appendix B. Using the simplified chemical model, we obtained a value consistent with that required from the observation although it was real. This model shows that the change of electron density in the observed gravity wave field arises mainly from the adiabatic change of temperature within the displaced parcels and the vertical transport of several neutral species. These neutrals have long photochemical lifetimes and participate in the reactions related to the loss and production of electrons in the displaced parcels. This originates in the fact that the time scale for the relaxation to photochemical equilibrium of electron density within vertically displaced air parcels is shorter than the period of the observed wave [*Hill and Bowhill*, 1979]. However, the scheme of chemical reactions related to the loss and production of electron is remarkably complicated in the lower *D* region [e.g., *Brasseur and Solomon*, 1986]. In these heights, hydrated cluster ions play an important role in the electron loss process. The recombination coefficient for clusters is faster than that for molecular ions but changeable. Consequently, it appears that the actual response of electrons to the observed gravity wave becomes much more complex than that described in Appendix B. The argument term of the response factor required from the observation may reflect the complexity of the chemical reaction in the lower *D* region.

In the comparison between the observation and the model calculation, we have shown that the enhancement of mesospheric echo is in a good agreement with the sharp gradient of the electron density produced by the observed gravity wave. This means that the vertical gradient of electron density is the greatest contributing factor in the mean gradient of potential refractive index in the mesosphere. From this point of view, specular echoes from the "ledge" structure in the *D* region are expected. HF echoes from this ledge have been reported by *Hocking and Vincent* [1982]. The height of the ledge is strongly affected by the temperature and shows a large variation (70–90 km) depending on the geophysical and seasonal conditions [*Arnold and Krankowsky*, 1977; *Arnold et al.*, 1980]. Such a seasonal variation in the height of the mesospheric echoing layer has been reported by *Balsley et al.* [1983], although they have suggested that the echoes arise from some kinds of instabilities of gravity waves and tide. Recently, it has been shown that the observed echo power enhancement is in reasonable agreement with the fluctuations in the electron density profile measured with a rocket [*Ulwick et al.*, 1988]. *Kelley and Ulwick* [1988] have suggested that the echo enhancement arises from the generation of neutral turbulence. However, it should be noted that in our experiment the echo enhancement is connected with the more stabilized region formed by the observed gravity wave rather than with the wave breaking. It will be an important work in the near future for VHF radar experiments to dis-

tinguish which is the primary cause of the echo enhancement in the mesosphere.

6. CONCLUSIONS

In this paper we have applied the Fresnel scattering model proposed by *Gage et al.* [1985] to clarify characteristics of mesospheric echoes observed by the MU radar at Shigaraki, Japan. In the extension of the model to mesospheric heights, the mean gradient of potential refractive index M_e applicable in the mesosphere was introduced in place of the stratospheric one used by *Gage et al.* [1985]. With this alteration we have shown that the extended Fresnel scattering model simulates very well the height profiles of echo power backscattered from the mesosphere. Provided that the spectrum of irregularities is independent of height, the observed echo power can be explained as due to the modulation of M_e by the simultaneously observed gravity wave. In the comparison between the observation and the model calculation, it has also been shown that the observed echo enhancement arises from sharp gradients of electron density which are formed by the observed gravity wave. Therefore we may expect intense backscattered echo from a region with the sharp gradient of electron density, for example, from the ledge structure in the D region.

APPENDIX A: MEAN GRADIENT OF POTENTIAL REFRACTIVE INDEX IN THE MESOSPHERE

We estimate here the mean gradient of the potential refractive index in mesospheric heights, defined as

$$M_e \equiv \Delta n/\Delta z \tag{A1}$$

where $\Delta n = n_P(z) - n(z)$ and the subscript P denotes quantities within vertically displaced parcels. The refractive index n is dominantly contributed by free electrons in the D region of the ionosphere, as shown in (3) in the text [e.g., *Balsley and Gage*, 1980]. This means that the refractive index is not conserved in an adiabatic process. Therefore when we evaluate the change of the refractive index in a vertically displaced air parcel, we must take into account the adiabatic change of electron number density in the parcel.

Consider first the change of neutral density in an air parcel which undergoes a vertical displacement from its equilibrium level. If the parcel is displaced by a small distance $\Delta z = z - z_0$ from the initial height z_0, the density in the parcel is given by

$$\rho_P(z) = \rho_P(z_0) + \delta\rho \tag{A2}$$

where $\delta\rho$ denotes the adiabatic change of the density due to the vertical displacement. Considering that the parcel conserves its potential temperature θ in the adiabatic process, we obtain

$$\delta\theta/\theta = (\delta p/\gamma p) - (\delta\rho/\rho) = 0 \tag{A3}$$

with the definition of θ,

$$\theta \equiv (p/\rho R)\{p(0)/p\}^{(\gamma-1)/\gamma} \tag{A4}$$

where R is the gas constant. With the aid of (A3) we see that (A2) can be rewritten as

$$\rho_P(z) = \rho_P(z_0) + (\delta p/c_s^2) \tag{A5}$$

where $c_s = (\gamma p/\rho)^{1/2}$ is the sound speed in the environmental atmosphere.

Similarly, we can represent the electron number density in the parcel displaced by Δz as

$$N_P(z) = N_P(z_0) + \delta N \tag{A6}$$

where δN denotes the adiabatic change of the electron number density in the parcel. Provided that the vertical displacement is due to either turbulence or small-scale waves with time scale much shorter than the chemical lifetime of electrons in the reaction process with ion and neutral species, the local equilibrium state is conserved during the displacement. Then, we can assume that the mixing ratio of electron number density to air number density in the parcel remains constant during the displacement. Therefore (A6) can be rewritten as

$$N_P(z) = N_P(z_0) + (N/\rho)(\delta p/c_s^2) \tag{A7}$$

with the aid of (A3). At the height z the difference between the electron number density in the displaced parcel and its environment is given by

$$\Delta N \equiv N_P(z) - N(z) = -N(z) + N_P(z_0) + \frac{N}{\rho}\frac{\delta p}{c_s^2} \tag{A8}$$

Noting in (A8) that $N_P(z_0) = N(z_0)$ and that the pressure in the parcel is reasonably assumed to be instantaneously adjusted to the environmental pressure during the displacement $p_P = p$ and then $\delta p = p(z) - p(z_0)$, we can easily show that

$$\Delta N/\Delta z = -(dN/dz) + (N/\gamma p)(dp/dz) \tag{A9}$$

Note that dN/dz and dp/dz in (A9) denote the mean gradients in the environmental atmosphere across the

TABLE 2. Reactions and Rate Coefficients in a Simplified Chemical Model

Reaction	Symbol	Rate Coefficient
$NO + h\nu \rightarrow NO^+ + e^-$	J	
$e^- + O_2 + M \rightarrow O_2^- + M$	β	$3.1 \times 10^{-31} (300/T)^{5/2}$ cm^6 s^{-1}
$O_2^- + O \rightarrow e^- + O_3$	γ_d	1.5×10^{-10} cm^3 s^{-1}
$H^+(H_2O)_n + e^- \rightarrow H + nH_2O$	α_d	$5 \times 10^{-6} (200/T)^{1/2}$ cm^3 s^{-1}
$X^+ + Y^- \rightarrow$ neutrals	α_i	6.0×10^{-8} cm^3 s^{-1}

turbulent layer. With the aid of (A9) and (3) in the text we find that (A1) can be written as (5) in the text.

APPENDIX B: RESPONSE OF ELECTRONS TO GRAVITY WAVES IN A SIMPLIFIED CHEMICAL MODEL

To give some meaning of the response factor F_R estimated in the text, we discuss here the response of electrons to the long-period gravity wave in the D region. In order to make a comprehensible discussion on the electron response, we limit the evaluation of the response factor to a height range around 70 km. At these heights the electron response can be discussed with a simplified chemical model. The chemical reactions used here are summarized in Table 2. In the simplified model we assume that NO^+ is rapidly converted to $H^+(H_2O)_n$ and that the photodetachment of O_2^- contributes poorly to the electron production. Around 70 km the relaxation time of electron to photochemical equilibrium in a vertically displaced air parcel is shorter than the period of the gravity wave considered here [*Hill and Bowhill*, 1979]. For simplicity we assume that the wave period is much longer than the time scale for the electron loss process due to the recombination.

We first consider the vertical transport of neutral species by the gravity wave. The perturbation in vertically displaced air parcels has been discussed by *Thrane and Grandal* [1981]. Considering neutral species with long chemical lifetimes, we see from the continuity equation for neutrals that the perturbation is given by

$$n_j'/\bar{n}_j = -(iw'/\omega H)[(1/\gamma) - (H/H_j)] \tag{B1}$$

where n_j denotes the jth neutral species and H_j is the scale height of $\bar{n}_j$ defined as

$$H_j \equiv -(1/\bar{n}_j)(\partial \bar{n}_j/\partial z) \tag{B2}$$

The temperature perturbation due to the wave is represented as

$$T'/\bar{T} = -(iw'/\omega H)[(\gamma - 1)/\gamma] \tag{B3}$$

Taking into account the chemical reactions summarized in Table 2, we see that the continuity equation for electrons is given by

$$\frac{\partial N}{\partial t} + \nabla \cdot (N\mathbf{v}) = \frac{J n_{NO}}{1+\eta} - (\alpha_d + \eta\alpha_i)N^2 \tag{B4}$$

where n_{NO} is the nitric oxide number density and η is the ratio of negative ions to the electron number density. Assuming the photochemical steady state for η, we can show that

$$\eta = \beta n_{O_2}^2/\gamma_d n_O \tag{B5}$$

Then, the perturbation of η can be represented as

$$\eta'/\bar{\eta} = (\beta'/\bar{\beta}) + 2(n_{O_2}'/\bar{n}_{O_2}) - (n_O'/\bar{n}_O) \tag{B6}$$

Also we obtain from (B4) that

$$N = (J n_{NO}/\eta\alpha_d)^{1/2} \tag{B7}$$

assuming the steady state for N. Then the perturbation of electrons is given by

$$N'/\bar{N} = (1/2)[(n_{NO}'/\bar{n}_{NO}) - (\alpha_d'/\bar{\alpha}_d) - (\eta'/\bar{\eta})] \tag{B8}$$

We neglected the perturbation of J in (B8) because of the transparency of the ionizing photons. Note that the perturbations of O_2 and O in (B6) and of NO in (B8) are given by (B1) because of their long lifetimes. With the aid of (B1), (B3), and (B6), and noting that $H_{O_2} = H$ and that α_d and β depend on temperature as shown in Table 2, we see that (B8) reduces to

$$N'/\bar{N} = -(iw'/\omega H)F_R \tag{B9}$$

where

$$F_R = \frac{1}{2}\left(\frac{2}{\gamma} + 5\frac{\gamma - 1}{\gamma} - \frac{H}{H_{NO}} - \frac{H}{H_O}\right) \tag{B10}$$

Thus we see that F_R depends on the height profiles of NO and O in this model. If we take $H_{NO} = H$ and $H_O = -2H/3$, we obtain $F_R = 1.7$. This value is consistent with the magnitude estimated from the observed echo profile. However, note that the O profile is much influenced by dynamical and chemical con-

ditions in the mesosphere [cf. *Brasseur and Solomon*, 1986]. We also see from (B10) that F_R becomes real in this simplified model. However, we may show that F_R becomes complex if the period of the observed gravity wave is not much longer than the time scale for the electron loss process due to the recombination in the more realistic model.

Acknowledgments. We thank the staff of the Shigaraki MU Observatory, the Radio Atmospheric Science Center, for their professional and technical support. Important discussions with M. Yamamoto are also acknowledged. One of the authors (Y.M.) also thanks T. Sato and H. Murata of Hyogo College of Medicine, and K. Kawahira of Toyama National College of Technology, for their useful suggestions and encouragement. The MU radar belongs to and is operated by the Radio Atmospheric Science Center, Kyoto University.

REFERENCES

Arnold, F., and D. Krankowsky, Ion composition and electron and ion-loss processes in the Earth's atmosphere, in *Dynamical and Chemical Coupling*, edited by B. Grandal and J. A. Holtet, pp. 93–127, D. Reidel, Hingham, Mass., 1977.

Arnold, F., D. Krankowsky, E. Zettwitz, and W. Joos, Strong temperature control of the ionospheric *D*-region: Evidence from in situ ion measurements, *J. Atmos. Terr. Phys.*, *42*, 249–256, 1980.

Austin, G. L., and A. H. Manson, On the nature of the irregularities that produce partial reflections of radio waves from the lower ionosphere (70–100 km), *Radio Sci.*, *4*, 35–40, 1969.

Balsley, B. B., and K. S. Gage, The MST radar technique: Potential for middle atmosphere studies, *Pure Appl. Geophys.*, *118*, 452–493, 1980.

Balsley, B. B., and R. Garello, The kinetic energy density in the troposphere, stratosphere, and mesosphere: A preliminary study using the Poker Flat MST radar in Alaska, *Radio Sci.*, *20*, 1355–1361, 1985.

Balsley, B. B., W. L. Ecklund, and D. C. Fritts, VHF echoes from the high-latitude mesosphere and lower thermosphere: Observations and interpretations, *J. Atmos. Sci.*, *40*, 2451–2466, 1983.

Brasseur, G., and S. Solomon, *Aeronomy of the Middle Atmosphere*, 452 pp., D. Reidel, Hingham, Mass., 1986.

Doviak, R. J., and D. S. Zrnic', Reflection and scatter formula for anisotropically turbulent air, *Radio Sci.*, *19*, 325–336, 1984.

Fukao, S., T. Sato, S. Kato, R. M. Harper, R. F. Woodman, and W. E. Gordon, Mesospheric winds and waves over Jicamarca on May 23–24, 1974, *J. Geophys. Res.*, *84*, 4379–4386, 1979.

Fukao, S., T. Sato, T. Tsuda, S. Kato, K. Wakasugi, and T. Makihira, The MU radar with an active phased array system, 1, Antenna and power amplifiers, *Radio Sci.*, *20*, 1155–1168, 1985*a*.

Fukao, S., T. Tsuda, T. Sato, S. Kato, K. Wakasugi, and T. Makihira, The MU radar with an active phased array system, 2, In-house equipment, *Radio Sci.*, *20*, 1169–1176, 1985*b*.

Gage, K. S., and B. B. Balsley, On the scattering and reflection mechanisms contributing to clear air radar echoes from the troposphere, stratosphere, and mesosphere, *Radio Sci.*, *15*, 243–257, 1980.

Gage, K. S., and J. L. Green, Evidence for specular reflection from monostatic VHF radar observations of the stratosphere, *Radio Sci.*, *13*, 991–1001, 1978.

Gage, K. S., B. B. Balsley, and J. L. Green, Fresnel scattering model for specular echoes observed by VHF radar, *Radio Sci.*, *16*, 1447–1453, 1981.

Gage, K. S., W. L. Ecklund, and B. B. Balsley, A modified Fresnel scattering model for the parameterization of Fresnel returns, *Radio Sci.*, *20*, 1493–1501, 1985.

Hill, R. J., and S. A. Bowhill, Relaxation to photochemical equilibrium of charged species within displaced air parcels in the *D*-region, *J. Atmos. Terr. Phys.*, *41*, 607–623, 1979.

Hocking, W. K., Measurement of turbulent energy dissipation rates in the middle atmosphere by radar techniques: A review, *Radio Sci.*, *20*, 1403–1422, 1985.

Hocking, W. K., Radar studies of small scale structure in the upper middle atmosphere and lower ionosphere, *Adv. Space Res.*, *7*, 327–338, 1987.

Hocking, W. K., and J. Röttger, Pulse length dependence of radar signal strengths for Fresnel backscatter, *Radio Sci.*, *18*, 1312–1324, 1983.

Hocking, W. K., and R. A. Vincent, A comparison between HF partial reflection profiles from the *D*-region and simultaneous Langmuir probe electron density measurements, *J. Atmos. Terr. Phys.*, *44*, 843–854, 1982.

Hodges, R. R., Jr., Generation of turbulence in the upper atmosphere by internal gravity waves, *J. Geophys. Res.*, *72*, 3455–3458, 1967.

Kelley, M. C., and J. C. Ulwick, Large- and small-scale organization of electrons in the high-latitude mesosphere: Implications of the STATE data, *J. Geophys. Res.*, *93*, 7001–7008, 1988.

Lindzen, R. S., Turbulence and stress owing to gravity wave and tidal breakdown, *J. Geophys. Res.*, *86*, 9707–9714, 1981.

Liu, C. H., Interpretation of MST radar returns from clear air, in *Handbook for MAP*, vol. 9, edited by S. A. Bowhill, pp. 49–56, Middle Atmosphere Program, University of Illinois, Urbana, 1983.

Muraoka, Y., K. Kawahira, T. Sato, T. Tsuda, S. Fukao, and S. Kato, Characteristics of mesospheric internal gravity waves observed by MU radar, *Geophys. Res. Lett.*, *14*, 1154–1157, 1987.

Muraoka, Y., T. Sugiyama, K. Kawahira, T. Sato, T. Tsuda, S. Fukao, and S. Kato, Formation of mesospheric VHF echoing layers due to a gravity wave motion, *J. Atmos. Terr. Phys.*, *50*, 819–829, 1988*a*.

Muraoka, Y., T. Sugiyama, K. Kawahira, T. Sato, T. Tsuda, S. Fukao, and S. Kato, Cause of a monochromatic inertia-gravity wave breaking observed by the MU radar, *Geophys. Res. Lett.*, *15*, 1349–1352, 1988*b*.

Ottersten, H., Mean vertical gradient of potential refractive index in turbulent mixing and radar detection of CAT, *Radio Sci.*, *4*, 1247–1249, 1969.

Röttger, J., Reflection and scattering of VHF radar signals from atmospheric refractivity structures, *Radio Sci.*, *15*, 259–276, 1980.

Röttger, J., VHF radar measurements of small-scale and mesoscale dynamical processes in the middle atmosphere, *Philos Trans. R. Soc. London, Ser. A.*, *323*, 611–628, 1987.

Röttger, J., and C. H. Liu, Partial reflection and scattering of VHF radar signals from the clear atmosphere, *Geophys. Res. Lett.*, *5*, 357–360, 1978.

Röttger, J., P. K. Rastogi, and R. F. Woodman, High-resolution

VHF radar observations of turbulence structures in the mesosphere, *Geophys. Res. Lett.*, *6*, 617–620, 1979.

Smith, S. A., D. C. Fritts, B. B. Balsley, and C. R. Philbrick, Simultaneous rocket and MST radar observation of an internal gravity wave breaking in the mesosphere, in *Handbook for MAP*, vol. 20, edited by S. A. Bowhill, pp. 143–146, Middle Atmosphere Program, University of Illinois, Urbana, 1986.

Smith, S. A., D. C. Fritts, and T. E. VanZandt, Evidence for a saturated spectrum of atmospheric gravity waves, *J. Atmos. Sci.*, *44*, 1404–1410, 1987.

Sugiyama, T., Response of electrons to a gravity wave in the upper mesosphere, *J. Geophys. Res.*, *93*, 11,083–11,091, 1988.

Tatarski, V. I., *Wave Propagation in a Turbulent Medium*, 285 pp., McGraw-Hill, New York, 1961.

Thrane, E. V., and B. Grandal, Observations of fine scale structure in the mesosphere and lower thermosphere, *J. Atmos. Terr. Phys.*, *43*, 179–189, 1981.

Ulwick, J. C., K. D. Baker, M. C. Kelley, B. B. Balsley, and W. L. Ecklund, Comparison of simultaneous MST radar and electron density probe measurements during STATE, *J. Geophys. Res.*, *93*, 6989–7000, 1988.

Wait, J. R., *Electromagnetic Waves in Stratified Media*, 608 pp., Pergamon, New York, 1970.

Yamamoto, M., T. Tsuda, S. Kato, T. Sato, and S. Fukao, A saturated inertia gravity wave in the mesosphere observed by the middle and upper atmosphere radar, *J. Geophys. Res.*, *92*, 11,993–11,999, 1987.

S. Fukao, S. Kato, T. Sato, and T. Tsuda, Radio Atmospheric Science Center, Kyoto University, Uji, Kyoto 611, Japan.

Y. Muraoka, Department of Physics, Hyogo College of Medicine, Nishinomiya, Hyogo 663, Japan.

T. Sugiyama, Department of Physics, Kyoto University, Kyoto 606, Japan.